

CHROM. 14,609

## DETERMINATION OF MACROPORE DIFFUSION IN MOLECULAR SIEVE PARTICLES BY PULSE GAS CHROMATOGRAPHY

A. BAIKER\* and M. NEW

*Swiss Federal Institute of Technology (ETH), Department of Industrial and Engineering Chemistry, CH-8092 Zurich (Switzerland)*

(Received October 20th, 1981)

---

### SUMMARY

The experimental conditions necessary for reliable determination of the intraparticle diffusivity of gases in porous solids by pulse gas chromatography (PGC) are investigated. Diffusivity measurements carried out with non-adsorbable tracer gases in packings of molecular sieve particles of different sizes indicate that the experimentally observed contributions of external mass transfer and intraparticle diffusion resistance may not depend on the particle size as theory predicts. With decreasing particle diameter the external mass transfer resistance becomes increasingly dominant as compared to intraparticle diffusion resistances. This finding follows from comparative experiments with packings of non-porous glass beads and porous molecular sieve particles of equal size. The sensitivity of the mass transfer rate parameter determination is markedly improved by using an experimental arrangement with a column to particle diameter ratio which corresponds to a "single pellet string reactor" (S.P.S.R.). The reliability of the determination of the intraparticle diffusivity with an S.P.S.R. has been checked by independent diffusivity measurements carried out on pressed single pellets of the molecular sieve. Steady-state counter-diffusion and dynamic pulse response measurements yielded an effective diffusivity comparable to that determined with the PGC method using an S.P.S.R. arrangement.

---

### INTRODUCTION

In the last decade, pulse gas chromatography (PGC) has gained acceptance as a rapid and versatile technique for the determination of the effective intraparticle diffusivity of gases in porous solids, *e.g.*, adsorbents and catalysts<sup>1-6</sup>. The reliability of the PGC technique for the determination of intraparticle diffusivity is strongly dependent on the experimental conditions under which the measurements are carried out<sup>7,8</sup>. The main objective of the present work is therefore to study the suitability of different experimental conditions for the determination of intraparticle diffusivity with the PGC technique and to check the diffusivity results obtained with independent measurements on single pellets in a diffusion cell.

## THEORY

The theory most often applied in recent years to the estimation of intraparticle diffusivity is generally referred to as the Kubin-Kucera model after the authors of the original papers<sup>9-11</sup> published in 1965. Initially, the model was applied to describe the dispersion of an adsorbable tracer gas pulse in a packed bed of porous adsorbent through which an inert gas is flowing. Later it was shown that the theory can also be applied if a non-adsorbable tracer is used. In this theory the moments of the chromatographic peak leaving the bed are related to the parameters describing the mass transfer process. An analytical solution of the Kubin-Kucera model is not possible in the time domain; however, solutions can be given in the Laplace or Fourier domains<sup>12</sup>. Moment expressions can be derived from these solutions in terms of various model parameters.

For a Dirac delta-input signal of a non-adsorbable tracer one obtains the following results for the first absolute,  $\mu_1$ , and second central moments,  $\mu'_2$  (ref. 1)

$$\mu_1 = (z/u) (1 + \delta_0) \quad (1)$$

$$\mu'_2 = 2 (z/u) \left[ \delta_1 + (E_A/z) (1 + \delta_0)^2 \cdot \frac{1}{u^2} \right] \quad (2)$$

where:

$$\delta_0 = \frac{1 - \alpha}{\alpha} \cdot \varepsilon \quad (3)$$

$$\delta_1 = \delta_e + \delta_i \quad (4)$$

The contribution of  $\delta_1$  to the second moment function (eqn. 2) is the sum of the external mass transfer,  $\delta_e$ , and the intraparticle diffusion contribution,  $\delta_i$ , which have different dependences on the average particle radius,  $R$ , of the packing:

$$\delta_e = \left( \frac{1 - \alpha}{\alpha} \cdot \varepsilon \right) \left( \frac{R^2 \varepsilon}{15} \right) \cdot \frac{5}{k_f R} \quad (5)$$

$$\delta_i = \left( \frac{1 - \alpha}{\alpha} \cdot \varepsilon \right) \left( \frac{R^2 \varepsilon}{15} \right) \cdot \frac{1}{D_c} \quad (6)$$

The first absolute and second central moments of the tracer concentration curve  $c(z,t)$  are defined as

$$\mu_1 = m_1/m_0 \quad (7)$$

$$\mu'_2 = \frac{1}{m_0} \int_0^{\infty} (t - \mu_1)^2 c(z,t) dt \quad (8)$$

where the integrals  $m_0$  and  $m_1$  are given by:

$$m_n = \int_0^{\infty} t^n c(z,t) dt \quad \text{for } n = 0, 1 \quad (9)$$

Eqn. 1 contains the bed length,  $z$ , the interstitial gas velocity,  $u$ , the particle porosity,  $\epsilon$ , and the column void fraction,  $\alpha$ , all of which can be measured independently of the chromatographic technique. This is not the case with the parameters determining the second moment given in eqn. 2. The axial dispersion,  $E_A$ , may be obtained from the slope of a plot of  $\mu_2^2$  against  $1/u^2$ ; however, the extraction of the effective intraparticle diffusivity,  $D_e$ , and of the fluid-particle mass transfer coefficient,  $k_f$ , from the intercept of this plot is difficult. Theoretically, it is possible to derive expressions for the third and higher moments in terms of these parameters. However, in practice, only zero, first and second moments are useful since higher moments can rarely be determined with appropriate accuracy from experimental response curves. An approach to avoid the application of higher moments is to calculate  $k_f$  from other approximate relations. Different expressions have been suggested<sup>13-16</sup> for the estimation of the fluid-particle mass transfer coefficient.

## EXPERIMENTAL

### Apparatus and procedure

The experimental arrangement employed is shown schematically in Fig. 1. It basically consists of three parts, the gas supply and control part, the test section (gas chromatographic column) and the data collection system.

The purity of the gases used in the experiments (He, Ar, N<sub>2</sub>) was better than

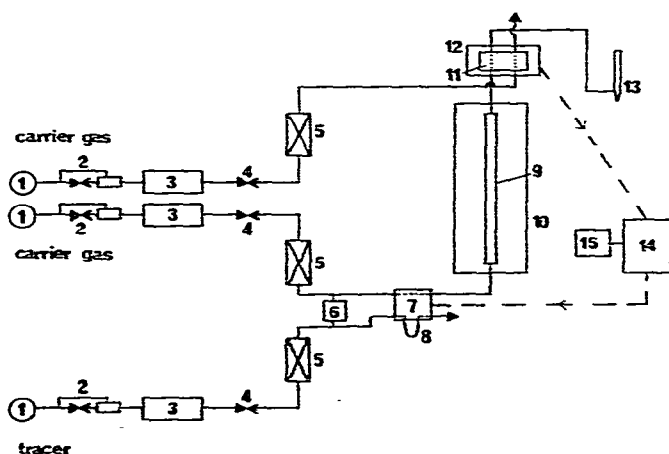


Fig. 1. Experimental arrangement used for pulse gas chromatography measurements. 1 = Gas cylinder; 2 = pressure controller; 3 = molecular sieve packing; 4 = low flow valve; 5 = flow meter; 6 = precision pressure gauge; 7 = tracer injection valve; 8 = sample loop; 9 = gas chromatographic column or single pellet string arrangement; 10 = temperature-controlled oven; 11 = hot-wire detector; 12 = detector heating block; 13 = soap bubble flow meter; 14 = PDP 11/10 process computer; 15 = x,y recorder.

99.99%, as quoted by the manufacturers. All gases were taken from commercial steel cylinders and dried before use by passing them through a packed bed of activated molecular sieve (Linde, 5A). The carrier gas flow-rates were controlled by a Dual GC Mass Flow Controller (Brooks Inst. Div., Model 5840). The tracer gas pulses were introduced by a COV Series eight-ports gas changeover valve (Mechanism Ltd.) equipped with two 0.15-cm<sup>3</sup> sampling loops. Pulses of pure gases were fed to the column inlet after it had been confirmed by varying the pulse inlet concentration that non-linearities due to concentration effects did not effect the experimental moment results.

The column (test section) was mounted in a gas chromatograph oven where the temperature could be held constant to within  $\pm 1^\circ\text{K}$ . Column lengths were determined before the tube was coiled and, from residence time measurements in the void column, the inner diameter of the tubing was determined to be 5.8 mm. The pressure drop in the column was measured by means of a high precision pressure difference gauge (Revue Thommen, Type 19 A2) and was at most 8% of the inlet pressure at the highest gas velocities reported.

The connection between the sample valve and the column as well as between the column end and the detector was of stainless-steel tubing (2 mm O.D.). To keep extra-column dispersion to a minimum, the length of all pulse-carrying tubing was kept as small as possible. By short-circuiting the column the system dead volume (including the sampling loop volume) was determined (1.07 cm<sup>3</sup>) and all first moment results reported below were corrected for holding times in the connecting lines. Contributions of the system dead volume and the constriction at the column outlet to the experimental second moments were ignored since they never exceeded 2%.

The detector was a Gow Mac Model 69-552. A bridge current of 140 mA was set and the detector bridge element was run at 420°K. The bridge element was controlled by means of a control unit (Carlo Erba, Model 230). The linearity of the detector response was periodically checked by means of an exponential dilution flask (Carlo Erba). Experimental tracer gas concentration functions were recorded with a PDP 11.10 process computer. The analogue detector control unit signal ranging between 0 and 10 V was divided down into equisized digitized levels between 0 and 4096. The response time, typically between 10 and 500 sec, was recorded at 2000 equally spaced but variable units of time.

### *Material*

Commercially available molecular sieve particles were employed for the measurements (Chemische Fabrik Uetikon, Type IG2-4Å). The physical properties of the porous particles were: surface area (BET), 12 m<sup>2</sup>/g; void fraction,  $\varepsilon = 0.305$ ; void volume,  $V_t = 0.252 \text{ cm}^3/\text{g}$ ; apparent density,  $\sigma_a = 1.30 \text{ g/cm}^3$ ; solid density,  $\sigma_s = 1.87 \text{ g/cm}^3$ . The solid density was measured in a helium pycnometer, and the apparent density by mercury displacement. The differential macropore size distribution measured with the mercury intrusion method is presented in Fig. 2. Before being packed into the column, the molecular sieve particles were kept in a vacuum-drying oven at 420°K and *ca.* 7 kPa for about 12 h. Prior to experimental runs the packed column was left overnight in the gas chromatograph oven at 420°K with inert carrier gas flowing. The packing porosity,  $\alpha$ , of the column was calculated from the apparent density of the particles and the bed bulk density.

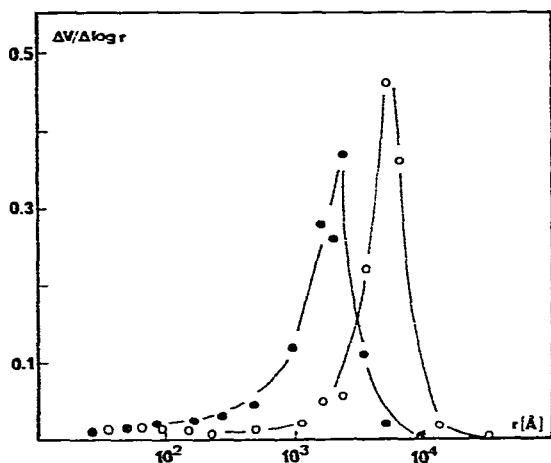


Fig. 2. Differential macropore size distribution of commercial (●) and pressed (○) molecular sieve pellets.

## RESULTS

### *Measurements with different ratios of column to particle diameter*

First the influence of the ratio of column to particle diameter on the determination of the mass transfer parameters was investigated. Experiments were carried out with four packings of different ratios of column to particle diameter ( $d_c/d_p$ ). The properties of the column packings of length 40 cm are given in Table I. Packings I and II consisted of well defined spherical particles as supplied by the manufacturer, whereas packings III and IV comprised crushed material of a less well defined shape. Pulse response experiments were carried out at  $T_1 = 313^\circ\text{K}$  and  $T_2 = 375^\circ\text{K}$  under a pressure of 100 kPa. Nitrogen was the carrier and argon the tracer gas. The interstitial carrier gas velocity range investigated with the four packings was 0.3–2 cm/sec. Fig. 3 shows a linearized plot of the experimentally observed dependence of first moments on the carrier gas flow-rate,  $F$ , for experiments carried out with packing IV. The plotted carrier gas flow-rates were measured at room temperature at the detector outlet. To calculate the interstitial gas velocity,  $u$ , under the experimental conditions this value was corrected for the effective column temperature assuming ideal gas behaviour. After this correction, identical slopes were obtained within the experimental error for the relation  $\mu_1$  vs.  $1/u$  for both temperatures and for the four different column packings. This result indicates that no marked adsorption was occurring in the system.

TABLE I

PROPERTIES OF MOLECULAR SIEVE PACKINGS EMPLOYED

Packing	Mesh size ( $\mu\text{m}$ )	$\alpha$	$d_c/d_p$
I	1870–2000	0.472	2.99
II	1000–1070	0.332	5.60
III	400– 430	0.404	13.97
IV	150– 200	0.412	33.14

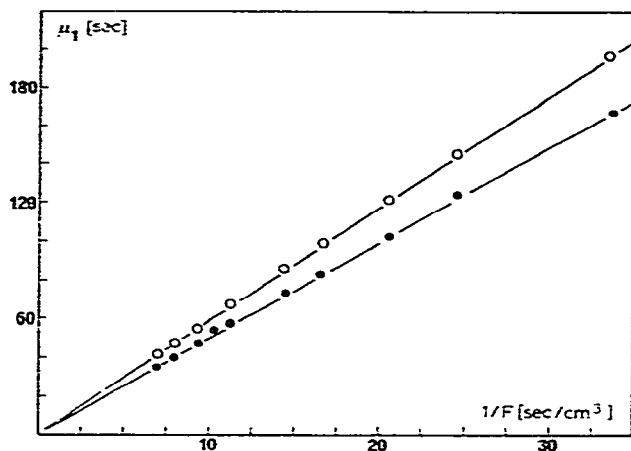


Fig. 3. Experimentally observed dependence of first moments,  $\mu_1$ , on the carrier gas flow-rate,  $F$ , for packing IV at 313 (○) and 375°K (●).

From the experimental first moments, intraparticle porosities were calculated applying eqns. 1 and 3. At  $T_1 = 313^\circ\text{K}$  the results for the four packings yielded a mean value of  $\varepsilon = 0.333$  and a 95% confidence interval of  $0.286 < \varepsilon < 0.380$ . The evaluation at  $T_2 = 375^\circ\text{K}$  gave a mean value of  $\varepsilon = 0.302$  and a 95% confidence interval of  $0.248 < \varepsilon < 0.355$ . These values are in good agreement with the values obtained from other determination methods, namely  $\varepsilon = 0.305$  from pycnometry and  $\varepsilon = 0.289$  from the relationship  $\varepsilon = V_1\sigma_a$ , with the total macropore volume  $V_1$  measured by mercury porosimetry.

Fig. 4 presents a linearized plot of the experimental second moments as a function of interstitial gas velocity. During the runs the interstitial carrier gas velocity was varied between 0.3 and 2.0 cm/sec. Within this interval eqn. 10

$$\mu_2/(2z/u) = \delta_1 + (E_A/x) (1 + \delta_0)^2 \cdot \frac{1}{u^2} \quad (10)$$

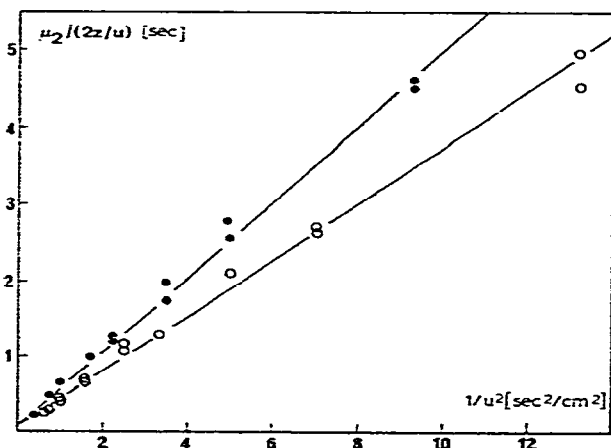


Fig. 4. Dependence of second moments on the interstitial carrier gas velocity,  $u$ , for packing IV at 313 (○) and 375°K (●).

TABLE II

AXIAL DISPERSION COEFFICIENTS AND RECIPROCAL TORTUOSITIES OF THE DIFFERENT MOLECULAR SIEVE PACKINGS (CF., TABLE I)

Packing	$T_1 = 313^\circ K$		$T_2 = 375^\circ K$	
	$E_A$ (cm <sup>2</sup> /sec)	$\eta$	$E_A$ (cm <sup>2</sup> /sec)	$\eta$
I	0.094	0.95	0.127	0.93
II	0.085	1.22	0.124	1.29
III	0.073	0.85	0.095	0.81
IV	0.069	0.79	0.096	0.80

(which is equivalent to eqn. 2) was accurate enough to account for the experimental observations. This was concluded from a statistical test for lack of fit which comprised the comparison of the residual sum of squares of the mathematical model with the experimental error. Applying eqn. 2, the axial dispersion coefficients given in Table II were calculated. The corresponding reciprocal packing tortuosity factors,  $\eta$ , calculated with eqn. 11

$$\eta = E_A/D_{AB}\alpha \quad (11)$$

are also listed in Table II. The molecular diffusion coefficients,  $D_{AB}$ , required for the calculation of  $\eta$  were obtained by the Chapman-Enskog relation<sup>17</sup>. The relatively large value of  $\eta$  obtained for packing II can be ascribed to packing inhomogeneities as is indicated by the low interparticle porosity,  $\alpha$ , measured for this packing (cf., Table I). The temperature dependence of the axial dispersion coefficients,  $E_A$ , presented in Table II is well described by a proportionality of  $T^{1.7}$  and indicates that the dispersion mechanism is close to a molecular one. A linear regression analysis employing eqn. 2 yielded the following values for the axial intercepts  $\delta_1$  for the four packings at  $T = 313^\circ K$  (values in parentheses are 95% confidence limits): packing I,  $\delta_1 = 0.146$  (0.09–0.20); packing II,  $\delta_1 = 0.049$  (0.01–0.08); packing III,  $\delta_1 = 0.048$  (–0.03–0.13); packing IV,  $\delta_1 = 0.119$  (0.03–0.21). The determined axial intercepts,  $\delta_1$ , do not depend on particle size as the theory predicts. Thus, the investigated experimental conditions (Reynolds number range,  $N_{Re} = 2uR/v \leq 3$ ; column to particle diameter ratio range,  $3 < d_p/d_c < 33$ ) are not suitable for a reliable determination of the effective intraparticle diffusion coefficient.

*Comparison of measurements in columns with porous and non-porous packing materials of similar mean particle sizes*

In order to find the reason for the behaviour observed with the packings of different particle sizes and to obtain some idea about the sensitivity of the PGC method for the determination of the intraparticle diffusivity, comparative measurements were carried out with packings of molecular sieve particles and non-porous glass beads of similar mesh sizes. Experiments were run at  $313^\circ K$  with four different carrier/tracer gas pairs in the carrier gas velocity range from 0.7 to 10 cm/sec. In the subsequent notation, He/Ar means that He was the carrier and Ar the tracer gas. The axial dispersion coefficients,  $E_A$ , for the porous and non-porous packings were de-

TABLE III

AXIAL DISPERSION COEFFICIENTS AND RECIPROCAL TORTUOSITIES OBTAINED WITH NON-POROUS AND POROUS PARTICLE PACKINGS

Gas pair	Mesh size 400–430 $\mu\text{m}$				Mesh size 1000–1070 $\mu\text{m}$			
	Glass bead packing ( $\alpha = 0.385$ )		Molecular sieve packing ( $\alpha = 0.458$ )		Glass bead packing ( $\alpha = 0.413$ )		Molecular sieve packing ( $\alpha = 0.376$ )	
	$E_A$ ( $\text{cm}^2/\text{sec}$ )	$\eta$	$E_A$ ( $\text{cm}^2/\text{sec}$ )	$\eta$	$E_A$ ( $\text{cm}^2/\text{sec}$ )	$\eta$	$E_A$ ( $\text{cm}^2/\text{sec}$ )	$\eta$
N <sub>2</sub> /He	0.176	0.59	0.226	0.64	0.205	0.64	0.361	1.23
N <sub>2</sub> /Ar	0.037	0.46	0.053	0.55	0.047	0.54	0.057	0.72
He/Ar	0.192	0.61	0.215	0.58	0.224	0.66	0.259	0.84
He/N <sub>2</sub>	0.197	0.66	0.215	0.61	0.221	0.69	0.258	0.89

terminated by a linear regression analysis with eqn. 2. The values obtained are summarized in Table III together with the reciprocal tortuosity factors calculated with eqn. 11. With all of the four gas pairs used the larger porous particle packing displays a higher dispersion than the corresponding non-porous packing. The comparison with the dispersion behaviour of the glass bead packings of different mesh sizes shows that the different dispersion behaviour of the two molecular sieve fractions cannot be exclusively due to the influence of the ratio of column to particle diameter. It seems that intraparticle diffusion is contributing to axial dispersion in the larger molecular sieve particle packing. The evaluation of molecular sieve intraparticle porosity from experimental runs with the packing of mesh size 1000–1070  $\mu\text{m}$  yielded the following  $\epsilon$  values with the different gas pairs employed: N<sub>2</sub>/He, 0.395; N<sub>2</sub>/Ar, 0.313; He/Ar, 0.338; He/N<sub>2</sub>, 0.347. The  $\epsilon$  values obtained with argon as tracer gas gave a slightly larger porosity if He was the carrier gas instead of N<sub>2</sub>. On the other hand the largest porosity is obtained when He is the tracer gas. Helium is capable of penetrating into the cavities of the molecular sieve, whereas the accessibility for N<sub>2</sub> (critical diameter 3 Å) and in particular Ar (critical diameter 3.84 Å) is strongly limited. The different accessibility affects the concentration distribution and the dispersion behaviour. The axial dispersion behaviour of the packing with the smaller molecular sieve particles is very similar to the one consisting of equally sized non-porous glass beads. For the latter there is no intraparticle diffusion contribution to the axial dispersion and, consistently, the intraparticle porosity,  $\epsilon$ , from first moment results with He as tracer gas, does not exceed those obtained with Ar and N<sub>2</sub>: N<sub>2</sub>/He,  $\epsilon = 0.344$ ; N<sub>2</sub>/Ar,  $\epsilon = 0.265$ ; He/Ar,  $\epsilon = 0.337$ ; He/N<sub>2</sub>,  $\epsilon = 0.343$ .

A more detailed analysis of the regression results obtained with eqn. 2 indicated that the assumption of a constant axial dispersion coefficient was valid only in the lower carrier gas velocity range investigated. This behaviour is illustrated in Fig. 5 which shows the deviation of the experimental and calculated second moment results,  $[\mu_2/(2z/u)_{\text{expt}} - \mu_2/(2z/u)_{\text{calc}}]$ , as a function of the carrier gas velocity for the experiments conducted with the molecular sieve packing of mesh size 1000–1070  $\mu\text{m}$ . A similar tendency was also observed for the other experiments carried out at carrier gas velocities up to 10 cm/sec. The introduction of a velocity-dependent axial dispersion coefficient according to eqn. 13 into eqn. 2 did not improve the quality of the fitting of the experimental results in the higher carrier gas velocity range as a comparison of the

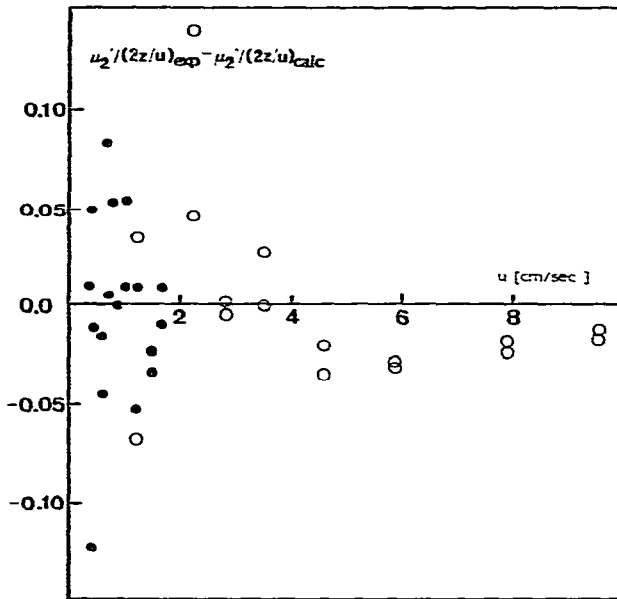


Fig. 5. Deviation between experimentally determined second moments and second moments calculated with eqn. 10 as a function of the interstitial carrier gas velocity,  $u$ , for the molecular sieve packing of mesh size 1000–1070  $\mu\text{m}$ . ●,  $\text{N}_2/\text{Ar}$ ,  $0.3 < u < 2.0$  cm/sec; ○,  $\text{N}_2/\text{Ar}$ ,  $0.7 < u < 10.0$  cm/sec.

residual sum of squares obtained for both models indicated. Consequently no statistically significant axial intercept,  $\delta_1$ , could be extracted for carrier gas velocities up to 10 cm/sec.

A definite conclusion concerning the influence of the intraparticle diffusion resistance on the tracer elution curve comes from a time domain regression analysis. Haynes<sup>8</sup> has derived eqn. 12 for the dispersion of a tracer pulse in a non-porous particle packing

$$E^* = \frac{1}{2} \left( \frac{\alpha N_1}{\pi t^{*3}} \right)^{0.5} \exp \left[ - \frac{(t^* - \alpha)^2 N_1}{4\alpha t^*} \right] \quad (12)$$

where  $t^* = tv/z$ ,  $v = u\alpha$  and  $N_1 = v/z/E_A$ ;  $E^*$  is the dimensionless residence time distribution function,  $v$  the empty column-based carrier gas velocity,  $z$  the packing length,  $N_1$  the axial Péclet number computed with the packing length and  $t$  the time. Haynes<sup>8</sup> showed that for  $N_1 > 100$  one observes a Gaussian distribution for the tracer elution curve in non-porous packings. Furthermore, he pointed out that porous and non-porous particle packings display an identical dispersion behaviour if the diffusion is rapid in both pore systems. For packings of porous particles one has to take into account both the interparticle and the intraparticle porosity in computing  $t^*$ . Eqn. 12 was applied to the experimental results obtained at 313°K for both the porous and the non-porous particle packings of mesh size 1000–1070  $\mu\text{m}$  with the gas pair He/Ar. The parameters  $v/z$  and  $N_1$  were determined by a non-linear regression analysis. Eqn. 12 fitted the results of both packing types equally well. By comparing

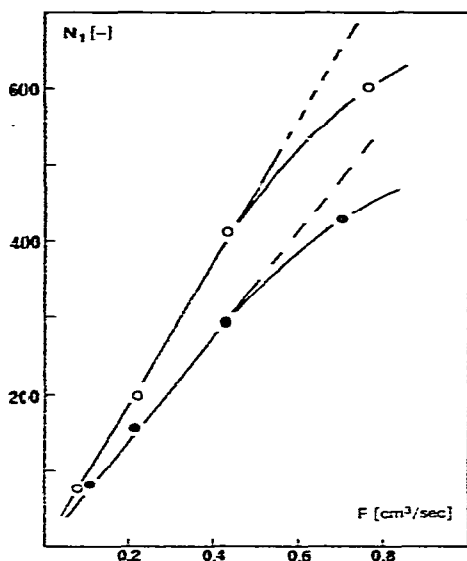


Fig. 6. Dependence of axial Péclet number,  $N_1$ , on carrier gas flow-rate,  $F$ , for glass bead packing (O) and molecular sieve packing (●) of mesh size 1000–1070  $\mu\text{m}$ .

the values of  $v_1 z$  for the porous and non-porous packings, an intraparticle porosity of  $\varepsilon = 0.314$  is estimated for the molecular sieve particles. This value agrees favourably with the value of 0.338 obtained from the first moment analysis.

Fig. 6 presents the dependence of the axial Péclet number on the carrier gas flow-rate for both packing types of mesh size 1000–1070  $\mu\text{m}$ . For both the porous and the non-porous packing one obtains, in the lower flow-rate range ( $F < 0.4 \text{ cm}^3/\text{sec}$ ), a linear relationship between the axial Péclet number and the carrier gas flow-rate. At higher carrier gas flow-rates the curves for both packing types depart from linearity, indicating a velocity-dependent axial dispersion coefficient. It is also seen that the porous molecular sieve particle packing displays a larger axial dispersion coefficient.

Edwards and Richardson<sup>18</sup> studied the gas dispersion in packed beds of non-porous particles over a wide range of particle sizes and Reynolds numbers. They correlated the observed axial dispersion coefficient with the normal gas diffusion coefficient and a velocity-dependent term according to eqn. 13:

$$E_A = 0.73 D_{AB} + \frac{uR}{1 + \frac{9.7 D_{AB}}{2uR}} \quad (13)$$

Employing eqn. 13 one can estimate a critical carrier gas flow-rate of about 0.4  $\text{cm}^3/\text{sec}$  for which the eddy diffusion contribution to the axial dispersion is less than 1%. This finding is in accordance with the results shown in Fig. 6 which indicate a velocity dependence of the axial dispersion at flow-rates larger than about 0.4  $\text{cm}^3/\text{sec}$ . Table IV shows a comparison of the experimentally determined and calculated second moments for both packing types. The second moments were calculated from the determined axial Péclet numbers with the assumption of a Gaussian distri-

TABLE IV

COMPARISON OF EXPERIMENTAL AND CALCULATED SECOND MOMENTS OBTAINED FOR NON-POROUS AND POROUS PACKINGS OF MESH SIZE 1000-1070  $\mu\text{m}$ 

<i>Glass bead packing</i>			<i>Molecular sieve packing</i>		
$F$ ( $\text{cm}^3/\text{sec}$ )	$\mu_{2,\text{calc}}'$ ( $\text{sec}^2$ )	$\mu_{2,\text{exptl}}'$ ( $\text{sec}^2$ )	$F$ ( $\text{cm}^3/\text{sec}$ )	$\mu_{2,\text{calc}}'$ ( $\text{sec}^2$ )	$\mu_{2,\text{exptl}}'$ ( $\text{sec}^2$ )
0.08	97.4	97.07	0.11	91.69	95.15
0.22	5.48	5.46	0.21	13.16	13.93
0.43	0.67	0.65	0.42	1.78	1.71
0.76	0.16	0.14	0.69	0.45	0.42

bution for the tracer concentration at the column end. The results listed in Table IV confirm that eqn. 12 describes the concentration distribution at the exit of both packed beds fairly well.

A comparison of the experimental runs with the porous molecular sieve particles and the non-porous glass beads indicates that under the given experimental conditions the intraparticle diffusion resistance in the molecular sieve particles could not be isolated in a significant way from axial dispersion influences. In order to investigate the influence of external mass transfer limitations on the determination of the effective intraparticle diffusivity,  $D_e$ , molecular sieve particles were used in an experimental set up corresponding closely to the single pellet string reactor (S.P.S.R.)<sup>19</sup>. With the S.P.S.R. external mass transfer influences should not play a major part since higher Reynolds numbers can be achieved in this arrangement. In addition, different correlations<sup>13-16</sup> are available from the literature to estimate the fluid-particle mass transfer coefficients in the Reynolds number range  $N_{\text{Re}} > 3$ . The experimental conditions and results of the S.P.S.R. runs are summarized in Table V. An estimation of the contribution of external mass transfer with the correlations given in ref. 13 indicated that the contribution of  $\delta_e$  to  $\delta_i$  was less than 5% for the S.P.S.R. runs reported. Thus, the intraparticle diffusivity,  $D_e$ , was calculated employing eqn. 4 with  $\delta_i = \delta_1$ . On the basis of this  $D_e$  value which has to be considered as a physical property of the molecular sieve, an expected contribution,  $\delta_{i,\text{ps}}$ , of the intraparticle

TABLE V

EXPERIMENTAL CONDITIONS AND RESULTS OF THE "SINGLE PELLETT STRING REACTOR" (S.P.S.R.) RUNS

<i>Experimental conditions</i>	<i>Results</i>
Carrier gas, He; tracer gas, Ar	$E_A = 0.365 \text{ cm}^2/\text{sec}$
Carrier gas velocity, $u$ 2.5-9.0 cm/sec	$\eta = 0.785$
Reynolds number range, $N_{\text{Re}} = 3-10$ ( $N_{\text{Re}} = 2Ru/v$ )	$D_e = 0.018 \text{ cm}^2/\text{sec}$ (0.012-0.024)
Pressure 1 bar	
Packing length 40 cm	
$d_c/d_p$ 1.97	
Mean particle size 0.294 cm	
Particle shape spherical	

TABLE VI

EXPECTED CONTRIBUTION,  $\delta_{i,PS}$  OF INTRAPARTICLE DIFFUSION RESISTANCE TO THE INTERCEPT,  $\delta_i$ , FOR MOLECULAR SIEVE PACKINGS

Packing mesh size ( $\mu\text{m}$ )	$\delta_{i,PS} \times 10^3$ (sec)	$\delta_{i,exptl}$ (sec)	95% confidence interval for $\delta_i$
1870-2000	4.87	0.146	0.09-0.20
1000-1070	2.51	0.049	0.01-0.08
400- 430	0.29	0.048	-0.03-0.13
150- 200	0.05	0.119	0.03-0.21

diffusion resistance could be calculated for the four packings of mesh sizes between 150 and 2000  $\mu\text{m}$ . using eqn. 6. The results of these calculations are given in Table VI, together with the experimental regression results and their 95% confidence limits.

With the exception of mesh size fraction 400-430  $\mu\text{m}$ , the experimental intercepts,  $\delta_{i,exptl}$ , differed significantly from zero. The calculated contributions,  $\delta_{i,PS}$ , based on  $D_e$  from the S.P.S.R. runs, are not included in the 95% confidence intervals of  $\delta_{i,exptl}$  for the remaining three packings. Since the carrier gas velocity range in these experiments corresponded to Reynolds numbers for which the usual relations for evaluating external mass transfer rate parameters are no longer valid, the Sherwood numbers,  $N_{Sh}$ , for external mass transfer

$$k_f = N_{Sh} D_{AB}/2R \quad (14)$$

were roughly estimated from the experimental results summarized in refs. 20 and 21. The estimated values for the Sherwood number are listed in Table VII together with the corresponding range of the Péclet number,  $N_{Pe}$ , defined as:

$$N_{Pe} = 2uR/D_{AB} \quad (15)$$

From the estimated Sherwood numbers the external mass transfer resistances,  $\delta_e$ , were calculated employing eqns. 5 and 14. The rough estimation of the Sherwood numbers led to  $\delta_e$  values which are more than an order of magnitude larger than the calculated  $\delta_{i,PS}$  from Table VI. Furthermore, these  $\delta_e$  values are well within the confi-

TABLE VII

ESTIMATES OF EXTERNAL MASS TRANSFER CONTRIBUTIONS TO THE INTERCEPT  $\delta_i$  FOR MOLECULAR SIEVE PACKINGS

Packing mesh size ( $\mu\text{m}$ )	Péclet number, $N_{Pe}$	Sherwood number, $N_{Sh}$	$\delta_e$ (sec)
1870-2000	0.5 -2.4	0.02	0.15
1000-1070	0.4 -2.0	0.01	0.08
400- 430	0.16-0.80	0.005	0.04
150- 200	0.07-0.33	0.001	0.03

dence intervals of the experimental  $\delta_{1,\text{exptl}}$  intercepts. This result supports the assumption that external mass transfer resistances were masking the intraparticle diffusion resistances in the molecular sieve particle packings of mesh size up to 2000  $\mu\text{m}$ .

*Determination of intraparticle diffusivity on single pellets in a diffusion cell*

In order to obtain some information about the reliability of the intraparticle diffusion coefficient determined with the PGC method, comparative diffusivity measurements were conducted on single molecular sieve pellets employing the steady state counter-diffusion<sup>22</sup> and the dynamic pulse-response methods<sup>23</sup>. The single pellets were pressed from crushed molecular sieve particles of diameters less than 100  $\mu\text{m}$ . The diffusion cell employed and the experimental procedure were the same as described elsewhere<sup>24</sup>. Three pressed pellets of different porosities,  $\varepsilon = 0.435, 0.356$  and  $0.325$ , were investigated. Fig. 2 presents the differential macropore size distributions of the commercial particles and of the pressed single pellet with  $\varepsilon = 0.435$ . The pore size distribution of the pressed pellet is shifted to larger pores; however, it shows the same characteristics as the one for the commercial particles.

Steady state counter-diffusion measurements were carried out with different counter-diffusing gas pairs. When using the gas pair A/B the concentration of gas B in the stream of gas A leaving the cell chamber was measured. The effective intraparticle diffusion coefficient,  $D_c$ , was computed from the measured diffusion flux  $N_A$  using eqn. 16

$$N_A = \frac{D_c P}{R_g T L \beta} \ln \left( \frac{1 - \beta y_{AL}}{1 - \beta y_{A0}} \right) \quad (16)$$

with

$$\beta = 1 + N_B/N_A = 1 - (M_A/M_B)^{0.5} \quad (17)$$

where  $P$  is the pressure,  $L$  the length of the cylindrical pellet,  $R_g$  the gas constant,  $y_{A0}$  and  $y_{AL}$  the mole fractions of A at the pellet ends and  $M_A, M_B$  the molecular weights of components A and B, respectively. The diffusivity results obtained with the steady-state counter-diffusion measurements are summarized in Table VIII. Employing eqn. 18

$$\bar{r} = \frac{1}{V_t} \int_0^{V_t} r dV \quad (18)$$

on the measured pore size distribution shown in Fig. 2 one can calculate an average macropore radius,  $\bar{r}$ , of 1950  $\text{\AA}$  for the commercial particles and a value of 4200  $\text{\AA}$  for the pressed pellet with  $\varepsilon = 0.435$ .

In cylindrical pores of this radius a transition region diffusion mechanism is most probable under the conditions given. The transition region diffusion coefficients,  $D_c$ , were calculated with eqn. 19

$$1/D_c = 1/D_{KA} + 1/D_{AB} \quad (19)$$

TABLE VIII

DIFFUSIVITY RESULTS OBTAINED WITH STEADY STATE COUNTER-DIFFUSION AND DYNAMIC PULSE RESPONSE MEASUREMENTS ON SINGLE MOLECULAR SIEVE PELLETS

Conditions		Diffusion coefficient (cm <sup>2</sup> /sec)	
Pellet	Gas pair	Steady state counter-diffusion	Dynamic pulse response
$\varepsilon = 0.435$	He/Ar	$D_{e,Ar} = 0.049$	$D_{e,Ar} = 0.054$ (0.036–0.073)
$\varepsilon = 0.435$	He/N <sub>2</sub>	$D_{e,N_2} = 0.059$	$D_{e,N_2} = 0.057$ (0.046–0.068)
$\varepsilon = 0.435$	N <sub>2</sub> /Ar	$D_{e,Ar} = 0.031$	
$\varepsilon = 0.356$	He/Ar	$D_{e,Ar} = 0.040$	$D_{e,Ar} = 0.040$ (0.034–0.046)
$\varepsilon = 0.356$	He/N <sub>2</sub>	$D_{e,N_2} = 0.046$	$D_{e,N_2} = 0.046$ (0.038–0.053)
$\varepsilon = 0.325$	N <sub>2</sub> /Ar	$D_{e,Ar} = 0.020$	

for the pressed pellet and the commercial IG2-4Å particles using a mean pore radius,  $\bar{r}$ , of 4200 Å and 1950 Å, respectively. The Knudsen diffusion coefficient  $D_{KA}$  in eqn. 19 is given by eqn. 20

$$D_{KA} = 9.7 \cdot 10^{-5} \bar{r} (T/M_A)^{0.5} \quad (20)$$

whereas the molecular diffusion coefficient is obtained from the Chapman–Enskog formula<sup>17</sup>. Employing eqn. 21

$$\psi = D_e \varepsilon / D_e \quad (21)$$

one obtains the following values for the tortuosity factors,  $\psi$ , depending on the gas pair: He/Ar,  $\psi = 4.2$ ; He/N<sub>2</sub>,  $\psi = 3.7$ ; N<sub>2</sub>/Ar,  $\psi = 2.5$ . The tortuosity factor, which should be a physical property of the porous material, depends on the employed gas pair. A similar trend is also observed when the “parallel path pore” model<sup>25</sup> is utilized to evaluate the tortuosity. The tortuosity factors obtained by employing this model are: He/Ar,  $\psi = 4.7$ ; He/N<sub>2</sub>,  $\psi = 3.6$ ; N<sub>2</sub>/Ar,  $\psi = 2.1$ . The smaller tortuosity factor resulting for the gas pair N<sub>2</sub>/Ar as compared with He/Ar is consistent with the results obtained in the gas chromatographic column arrangement, where a larger intraparticle porosity was found with the gas pair He/Ar than with N<sub>2</sub>/Ar. The steady state diffusion results with molecular sieve pellets of different porosities given in Table VIII indicate that the assumption of a constant, but gas pair-dependent tortuosity factor is reasonable in the investigated porosity range  $0.325 < \varepsilon < 0.436$ .

The pellets with porosities of  $\varepsilon = 0.435$  and  $0.356$  were also investigated by the dynamic pulse response method described by Dogu and Smith<sup>23</sup>. For the first normalized moment,  $\mu_{1,corr}$  of the pellet itself, *i.e.*, the net diffusion time without any dead volume contributions, these authors derived eqn. 22:

$$\mu_{1,corr} = \frac{L^2 \varepsilon (3QD_e/L + F_2)}{6D_e (QD_e/L + F_2)} \quad (22)$$

Here  $Q$  is the area of the end face of the pellet and  $F_2$  the carrier gas flow-rate on the

pellet side which is connected to the detector. Eqn. 22 was applied to the experimentally determined first moments after these were corrected for dead volume contributions. The intraparticle diffusion coefficients,  $D_e$ , were obtained by a non-linear regression analysis of eqn. 22. The diffusivity results obtained at 313°K and 100 kPa are given in Table VIII together with their 95% confidence limits as obtained from the non-linear regression analysis. A comparison of these values with the diffusivities measured by the steady state method indicates that the dynamic results are not significantly different.

From the diffusion cell results obtained with He/Ar one can estimate an effective intraparticle diffusivity,  $D_e = 0.022$ , for the commercial molecular sieve particles. This value is calculated from eqn. 20 with the tortuosity factor  $\psi = 4.2$  obtained for this gas pair and the structure parameters ( $\epsilon = 0.305$ ,  $\bar{r} = 1950 \text{ \AA}$ ) measured for the commercial IG2-4Å pellets. It is comparable to the intraparticle diffusivity determined with the PGC method in the S.P.S.R. arrangement ( $D_e = 0.018$ ; 95% confidence limits 0.012–0.024). These results confirm that the macropore diffusivity of molecular sieve particles can reliably be determined by the PGC method if an S.P.S.R. arrangement is employed and the tracer gas used has a critical diameter which excludes penetration into the micropores.

## CONCLUSIONS

The present investigation has shown that for reliable determination of intraparticle diffusion coefficients by the pulse gas chromatographic method there are definite limits with respect to the ratio of column to particle size. The frequently postulated simplifying assumption of a negligible external mass transfer resistance becomes doubtful with decreasing particle size. In addition, the mass transfer resistance term,  $\delta_1$ , in the Kubin–Kucera model tends to become very small with decreasing particle size, leading to values which are experimentally difficult to detect. Pulse gas chromatography measurements carried out in an experimental arrangement with a column to particle diameter ratio corresponding to a "single pellet string reactor" yielded an effective intraparticle diffusivity which is comparable to the values obtained by steady-state counter-diffusion and dynamic pulse response measurements on single pressed pellets in a diffusion cell.

## ACKNOWLEDGEMENT

The Swiss National Science Foundation is acknowledged for financing this work.

## REFERENCES

- 1 R. L. Cerro and J. M. Smith, *AIChE J.*, 16 (1970) 1035.
- 2 Yi Hua Ma and C. Mancel, *AIChE J.*, 18 (1972) 1149.
- 3 W. R. Mac Donald and H. W. Habgood, *Can. J. Chem. Eng.*, 50 (1972) 462.
- 4 H. W. Haynes, Jr. and P. N. Sharma, *AIChE J.*, 19 (1973) 1043.
- 5 N. Hashimoto and J. M. Smith, *Ind. Eng. Chem., Fundam.*, 13 (1974) 115.
- 6 P. N. Sharma and H. W. Haynes, Jr., *Advan. Chem. Ser.*, 133 (1974) 205.
- 7 S. K. Gangwal, R. R. Hudgins and P. L. Silveston, *Can. J. Chem. Eng.*, 56 (1978) 554.

- 8 H. W. Haynes, Jr., *Chem. Eng. Sci.*, 30 (1975) 955.
- 9 M. Kubin, *Collect. Czech. Chem. Commun.*, 30 (1965) 1104.
- 10 M. Kubin, *Collect. Czech. Chem. Commun.*, 30 (1965) 2900.
- 11 E. Kucera, *J. Chromatogr.*, 19 (1965) 237.
- 12 P. Schneider and J. M. Smith, *AIChE J.*, 14 (1968) 762.
- 13 N. Wakao and T. Funazkri, *Chem. Eng. Sci.*, 33 (1978) 1375.
- 14 L. J. Petrovic and G. Thodos, *Ind. Eng. Chem. Fundam.*, 7 (1968) 274.
- 15 W. E. Ranz and W. R. Marshall, *Chem. Eng. (Prague)*, 48 (1952) 173.
- 16 P. N. Dwivedi and S. N. Upadhyay, *Ind. Eng. Chem. Proc. Des.*, 16 (1977) 157.
- 17 J. O. Hirschfelder, C. F. Curtiss and R. B. Bird, *Molecular Theory of Gases and Liquids*, Wiley, New York, 1954.
- 18 M. F. Edwards and J. F. Richardson, *Chem. Eng. Sci.*, 24 (1969) 1741.
- 19 D. S. Scott, W. Lee and J. Pappa, *Chem. Eng. Sci.*, 29 (1974) 2155.
- 20 H. Martin, *Chem. Eng. Sci.*, 33 (1978) 913.
- 21 P. A. Nelson and T. R. Galloway, *Chem. Eng. Sci.*, 30 (1975) 1.
- 22 E. Wicke and R. Kallenbach, *Kolloid-Z.Z. Polym.*, 17 (1941) 135.
- 23 G. Dogu and J. M. Smith, *AIChE J.*, 21 (1975) 58.
- 24 M. New, A. Baiker and W. Richarz, *Chem.-Ing.-Tech.*, 51 (1979) 972.
- 25 M. F. L. Johnson and W. E. Steward, *J. Catal.*, 4 (1965) 248.